AAPS PharmSciTech (2022) 23:284
https://doi.org/10.1208/s12249-022-02437-z

RESEARCH ARTICLE

Advancements in Amorphous Solid Dispersions to Improve Bioavailability

Drug-Carrier Miscibility in Solid Dispersions of Glibenclamide and a Novel Approach to Enhance Its Solubility Using an Effervescent Agent

Muralidhar Pisay[1] · K. Vijaya Bhaskar[2] · Chetan Hasmukh Mehta[1] · Usha Yogendra Nayak[1] · Kunnatur Balasundara Koteshwara[1] · Srinivas Mutalik[1]

Received: 22 July 2022 / Accepted: 4 October 2022 / Published online: 17 October 2022

Abstract

The present research aims to investigate the miscibility, physical stability, solubility, and dissolution rate of a poorly water-soluble glibenclamide (GLB) in solid dispersions (SDs) with hydrophilic carriers like PEG-1500 and PEG-50 hydrogenated palm glycerides (Acconon). Mathematical theories such as Hansen solubility parameters, Flory Huggins theory, Gibbs free energy, and the *in silico* molecular dynamics simulation study approaches were used to predict the drug-carrier miscibility. To increase the solubility further, the effervescence technique was introduced to the conventional solid dispersions to prepare effervescent solid dispersions (ESD). Solid dispersions (SDs) were prepared by microwave, solvent evaporation, lyophilization, and hot melt extrusion (HME) techniques and tested for different characterization parameters. The theoretical and *in silico* parameters suggested that GLB would show good miscibility with the selected carriers under certain conditions. Intermolecular hydrogen bonding between the drug and carrier(s) was confirmed by Fourier transform infrared spectroscopy and proton nuclear magnetic resonance spectroscopy. Solid-state characterizations like powder X-ray diffraction, differential scanning calorimetry, and microscopy confirm the amorphous nature of SDs. The addition of the effervescent agent improved the amorphous nature, due to which the solubility and drug release rate was increased. *In vitro* and *ex vivo* intestinal absorption studies showed improved flux and permeability than the pure drug, suggesting an enhanced drug delivery. The GLB solubility, dissolution, and stability were greatly enhanced by the SD and ESD technology.

Keywords effervescence · *in silico* and theoretical solubility and miscibility · *in vitro-ex vivo* correlation · stability

Introduction

The novel chemical molecules show improved affinity toward the target receptors. To achieve this, the lipophilicity of the compounds should be increased. As a result, the balance between the hydrophilic and the lipophilic nature is disturbed. Finally, this leads to reduced oral bioavailability [1]. To maintain the balance between these two, solubility should be improved. Many researchers have extensively tried size reduction, salt formation, prodrug, complexation, emulsification, etc., to enhance solubility [2]. Though these techniques successfully improved the solubility of the drug molecules, they failed to maintain the supersaturation state in the dissolution media. The supersaturation state helps in increasing the permeability of drug molecules and also prevents crystallization of the drug in the dissolution media. Converting the crystalline drug to the amorphous form can solve the stated issue. Solid dispersion (SD) is an old technique that improves solubility by increasing the amorphous nature. However, due to the successful maintenance of the supersaturation state, SDs are still attracting the interest of

✉ Kunnatur Balasundara Koteshwara
kb.koteshwara@manipal.edu

✉ Srinivas Mutalik
ss.mutalik@manipal.edu

[1] Department of Pharmaceutics, Manipal College of Pharmaceutical Sciences, Manipal Academy of Higher Education, Manipal, Karnataka State 576106, India

[2] Department of Pharmaceutical Chemistry, Manipal College of Pharmaceutical Sciences, Manipal Academy of Higher Education, Manipal, Karnataka State 576104, India

researchers. SDs are formulated using various methods by dispersing the hydrophobic drug in a hydrophilic carrier. These carrier(s) used in the preparation have solubilizer and stabilizer properties. The carrier shows the stabilizer property by inhibiting molecular mobility, enhancing energy activation, and increasing the glass transition temperature [2].

To prepare the stable SDs, the drug and polymer(s) should be miscible by obeying the thermodynamics law. This will prevent amorphous phase separation and recrystallization in the supersaturation state. At the same time, to formulate the SDs, extreme conditions like temperature, pressure, radiation, and organic solvents will be used. It may lead to amorphous phase separation and recrystallization upon storage. To prevent this, it is essential to examine the drug and carrier(s) miscibility at room temperature [3].

The *in silico* molecular dynamics (MD) simulation tool explains the chemical and physical interaction between the drug and the carrier. MD also gives information about the preformulation and post-formulation properties [4]. This information might reduce the production cost with inbuilt quality. The MD simulation works by various principles, but the most accepted one is the Hildebrand solubility parameter approach [4]. On the other hand, mathematical theories like the Hansen solubility parameter [5], Flory-Huggins miscibility parameter [6], and Gibb's free energy calculation [7] explain the drug's miscibility and selected carriers even at room temperature.

Glibenclamide (GLB) is one of the widely prescribed anti-diabetic drugs. It comes under the sulfonylureas chemical class and belongs to the BSC-II with low aqueous solubility and high membrane permeability, with pKa 4.32 [8]. GLB showed higher absorption in basic pH. The reported solubility of GLB is 0.04 mg/mL in water.

PEG 1500 is a solubilizer, showing its activity in a polar solvent by forming the non-ionic micelles around the hydrophobic. Thus, the solubility of poorly water soluble drugs will be enhanced. Due to its non-ionic surfactant property, PEG-1500 will also increase the permeability of molecules across the cell membrane since the unionized chemicals will easily cross the membrane compared to ionized drugs [9]. Acconon C-50 is a polymeric fatty acid surfactant that has PEG 1500 with palmitic acid. Acconon also enhances the solubility of poorly soluble drugs by micellar formation. The micelles formed by Acconon C-50 are highly unionized. Therefore, permeability across the cell membrane is high in formulations prepared using Acconon C-50. Since PEG 1500 and Acconon C-50 have solubilizer properties, these two carriers can increase the aqueous solubility of poorly water-soluble drugs [10]. This may also improve the permeability by producing smaller particles with a more effective surface area.

In the present work, we adopted effervescence technology to prepare the SDs. The effervescence approach is widely used in pharmaceutical formulations like gastro retentive drug delivery systems and antacid preparations. This technique has also been proven to improve the drug's oral bioavailability. Effervescence technology works by producing gas upon exposure to moisture. Introducing this phenomenon to SDs will result in effervescence induced solid dispersions (ESD), which might increase the amorphous nature, solubility, and dissolution rate of the conventional SDs [11, 12].

Materials and Methods

GLB was received from Sun Pharmaceutical Industries Ltd, Mumbai, India, as a gift. Polyethylene glycol (PEG) 1500 was from Unitop Chemicals Private Limited, Mumbai, India, and Acconon C-50 was given as a gift sample from the ABITEC Corporation, Mumbai, India. Other chemicals and solvents were purchased from Finar Limited, Ahmedabad, India.

Computational Method for Solubility Parameter Calculation

The material science suite in the Schrodinger software was used to conduct the Molecular Dynamics simulation study. Chemical structures of the drug and Acconon C-50 [10] were drawn using the 2D sketcher tool and then converted into the 3D format with an inbuilt maestro interface. The LigPrep module with OPLS3 was used in energy minimization and structural optimization. PEG 1500 structure was drawn using the inbuilt polymer builder tool. The hydrogen atom was selected as the initiator and terminator group, and the monomer was sketched by mentioning the monomer composition. The drug, Acconon C-50, and PEG 1500 structures were built at pH 7. The disorder system was developed by 1:1 molar ratio of GLB and carrier(s). The steep set descent was used to minimize the molecular mechanic framework with a 1.0 Kcal/mol/A° 2000 merging threshold and allow 2000 maximum interactions. MD simulation was run at 1 bar pressure at 300 K for 10ns with an NPT ensemble [4, 13].

GLB-Carrier Miscibility

The miscibility between the drug and selected carrier(s) was theoretically calculated by the Hansen solubility parameter, Flory-Huggins interaction parameters, and Gibbs free energy calculations.

i. Hansen Solubility Parameter Estimation

The solubility parameter (δ) is the sum of the cohesive interactions, i.e., the dispersion forces (δ_d), polar forces (δ_p), and cohesive forces (δ_h) among the molecules in a mixture [14].

The following equation was used to calculate the solubility parameter:

$$\delta = \sqrt{\left(\delta_d^2 + \delta_p^2 + \delta_h^2\right)}. \quad (1)$$

The δ_d, δ_p, δ_h can be calculated by following formulas:

$$\boldsymbol{\delta_d} = \frac{\boldsymbol{\varepsilon F_d}}{\boldsymbol{V}} \quad (2)$$

$$\boldsymbol{\delta_p} = \frac{\sqrt{\left(\boldsymbol{\varepsilon F_p^2}\right)}}{\boldsymbol{V}} \quad (3)$$

$$\boldsymbol{\delta_h} = \frac{\boldsymbol{\varepsilon E_h}}{\boldsymbol{V}} \quad (4)$$

where, F_d,F_p are molar attraction forces of dispersive interaction, dipole-dipole interaction, and E_h is hydrogen bonding forces.

ii. Flory-Huggins Interaction Parameters (*x*)

GLB and carrier(s) physical mixture was prepared in the ratio of 100:0, 80:20, 60:40, 40:60, and 20:80, and its melting point depression was measured using the following equation to get the Flory-Huggins interaction parameters (***x***) [6].

$$\left(\frac{\mathbf{1}}{\boldsymbol{T_m}} - \frac{\mathbf{1}}{\boldsymbol{T_m^o}}\right) = \frac{\boldsymbol{-R}}{\boldsymbol{\Delta HF}}\left(\ln \varnothing_d + \left(\mathbf{1} + \frac{\mathbf{1}}{\boldsymbol{m}}\right) x \varnothing^2 \boldsymbol{p}\right) \quad (5)$$

where,

$\boldsymbol{T_m}$ and $\boldsymbol{T_m^o}$ are the melting point of the drug-carrier physical mixture and pure drug. $\boldsymbol{\Delta HF}$ is the heat of the fusion of the drug, $\varnothing_d$,$\varnothing_p$ are the volume fraction of drug and polymer. To get the ***x*** value, a graph was plotted against $\varnothing^2\boldsymbol{p}$Vs $\left(\frac{1}{T_m} - \frac{1}{T_m^o}\right)\frac{\Delta HF}{-R} - \ln\varnothing_d - \left(1 - \frac{1}{m}\right)\varnothing_p$. The slope of the obtained best-fit equation is the ***x*** value [14].

iii. Gibb's Free Energy Calculation

As explained in the Flory-Huggins interaction parameters (***x***), the melting point depression method was used to calculate Gibb's free energy using the following formula [7, 14]:

$$\frac{\boldsymbol{\Delta G_{mix}}}{\boldsymbol{RT}} = \varnothing_d \times \ln\varnothing_d + \frac{\varnothing_p}{\boldsymbol{m}} \times \ln\varnothing_p + \varnothing_d\varnothing_p \quad (6)$$

where,

$\boldsymbol{\Delta G_{mix}}$ is the Gibbs free energy and ***m*** is the molecular weight of the carrier divided by the molecular weight of the drug.

Preparation of SD and ESD

To prepare SDs, GLB and carrier(s) were taken in 1:1 molar ratio. ESDs were formulated by taking GLB, carrier(s), and effervescent agent in the molar ratio of 1:1:0.5. To create the effervescent nature, sodium bicarbonate (3 moles) was added to one mole of citric acid. The solid dispersions were prepared by microwave, solvent evaporation, lyophilization, and hot-melt extrusion techniques [14]. The solubility and drug release profile of SDs prepared by these four methods were compared.

Microwave Method

To prepare SDs in the microwave method physical mixture containing GLB, carrier (s), and effervescent agent (for ESDs) was prepared in above mentioned ratios. The physical mixture was placed in the IFB 25L domestic microwave. The instrument was set to maximum power, and the process was continued for 60 s. The molten mass was cooled and stored in an air-tight container [15].

Solvent Evaporation (SE) Method

GLB (10 mg) was dissolved in 5 mL of methanol using bath sonication. To this, equal molar volume carrier(s) was added, and the bath sonication was continued to get a clear mixture of drug and carrier. To prepare ESD, the effervescent agent was added to the clear mix of drug, carrier, and sonication was continued to get the clear blend. At 50°C temperature, methanol was allowed to evaporate. The prepared SDs were collected and stored for further use [16].

Lyophilization Method

Firstly, 10 mg of GLB was dissolved in 5 mL methanol, and an equimolar amount of carrier(s) was separately dissolved in water. These two solutions were mixed to get a clear solution. To prepare ESDs, the effervescent agent was added to the methanol drug mixture, and the carrier mixture was added. This clear mixture(s) was kept at −80°C in the New Brunswick ultra-low temperature freezer to freeze. The frozen samples were processed in the Freeze-dryer Alpha 1-2 LD Plus for 48 h [17].

Hot-Melt Extrusion Method (HME)

In a glass mortar, 15 g of GLB, carrier(s), and effervescent agent (for ESDs) were mixed gently with a glass pestle to prepare the physical mixture. This physical mixture was processed in OMICRON 10 PHARMA co-rotating twin-screw extruder (Steer Engineering, Bangalore, India) with a 1.71-mm screw diameter at 105 RPM. The barrels were set at

40°C (B1), 100°C (B2), 174°C (B3), and 85°C (B4). The obtained product was dried at room temperature [18].

Solid-State Characterization

Thermal Analysis

In an aluminum cup, 3–8 mg of GLB, PEG 15000, Acconon C-50 carrier(s), drug-carrier physical mixtures, and SDs were taken and closed with an aluminum lid crimped. The crimped sample was placed in the Shimadzu-DT-60 differential scanning calorimeter (DSC) by taking the pre-crimped empty aluminum cup as a blank. Nitrogen gas at 40 mL/min flow was supplied to create the *in situ* inert environment. To get the thermograms, the samples were analyzed at 25–250°C at 10°C/min [8].

Powder X-ray Diffraction

The diffractograms were recorded for pure drug and SDs using the Rigaku Miniflex 600 X-Ray Diffractometer. The instrument has an X-ray generation capacity of up to 40 kV and a 50–130° wide-angle measurement to measure the 2θ value. The nickel filters were used to pass the single beam of X-rays. The measurement was done at room temperature with a 15-mA voltage. The samples (10–20 mg) were analyzed at the 5–40 2θ range to record the diffractogram [14].

Fourier Transform Infrared Spectroscopy

The Fourier transform infrared spectroscopy (FTIR) spectra for the individual samples of GLB, carriers, GLB-PEG 1500, and GLB-Acconon C-50 physical mixtures, and SDs were acquired after scanning at a wavenumber range of 400–4000 cm^{-1}. For this purpose, the Alpha II compact attenuated total reflectance-Fourier transform infrared (ATR-FTIR) spectrometer (Bruker, US) was used. Firstly, the zinc selenide crystal was cleaned using isopropanol, and the blank correction was done. A small micro-spatula portion (15–20 mg) of the solid sample was placed over it to cover the ATR crystal. The anvil was gently pressed down till it contacted the sample. The anvil arm was rotated to ensure complete contact between the sample and crystal [19].

Proton Nuclear Magnetic Resonance (1H NMR)

The Bruker ASCEND TM 400 NMR analyzer Billerica, MA, USA, was used to study the possible molecular interaction between the drug and selected carrier(s). A clear solution of drug and SDs was prepared using deuterated chloroform [19].

Polarized Optical Microscopy

The polarized optical microscopic images were taken using the polarizing optical microscope (POM) (PM-VM-2727, SDTech Equipements, Mumbai, India). Approximately 5 mg of sample (drug or prepared SDs) was taken on a cleaned glass slide, kept on a hot plate, and allowed to melt. A glass coverslip was taken and covered the molten mass. The glass slide was allowed to cool down to room temperature and placed under the POM to visualize the crystalline properties [20].

Microscopic Examination

The morphology of the prepared samples was analyzed primarily by the motic light microscope. Before starting the analysis, the motic light microscope was adjusted to get the optimum lighting and connected to the system. A pinch of the sample was taken on a clean glass slide and spread. The motic live imaging software was used to capture the images.

To confirm the results obtained from the motic microscope, the EVO MA18 with Oxford EDS (X-act) scanning electronic microscope (SEM) (Gemini SEM 300-820201722) was used. The samples were stuck to the glass slide with a double-sided adhesive carbon tape and connected to the gold sputtering under a vacuum. This sample slab assembly was placed on the sample chamber of the scanning electronic microscope at a 10-mm working distance. To create the inert environment, 99.99% pure liquid nitrogen was supplied with a low vacuum voltage of 30 kV. At a depth of 1000× magnification, the samples were analyzed. The instrument was maintained at 21–24°C with 60% RH [8].

Solubility Studies

An excess amount of drug or SDs was added to the phosphate buffer pH 6.8, 7.4 pH 1.2 acidic buffer to maintain the supersaturated condition. This mixture was kept for stirring in a tube rotator at 50 rpm for 24 h. At the end of mentioned time, the samples were centrifuged for 10 min at 10,000 rpm to separate the supernatant. The collected supernatant solutions were analyzed by the RP-HPLC method using LC 2010 HT (Shimadzu, Kyoto, Japan) RP HPLC system with Chromosol JADE C18 column as a stationary phase. Acetonitrile (ACN):water (60:40; adjusted to pH 2.5 with orthophosphoric acid) was the mobile phase. The flow rate was 1.4 mL/min, and 236 nm was the maximum wavelength (λ max) [21].

Dissolution Studies

Dissolution for GLB and prepared SDs were performed in the Electrolab Dissolution Tester, Electrolab India Pvt. Ltd.,

Mumbai, India. For this purpose, the phosphate buffer of pH 6.8, 7.4, and pH 1.2 acidic buffer was used as a dissolution medium. The dissolution was performed at 37±0.5°C and 75 RPM for 90 min. At regular intervals, 5 mL of the sample(s) was collected and immediately replaced with the fresh dissolution media. The collected samples were stored for further analysis [21].

In Vitro Diffusion Studies

Before starting the study, a dialysis membrane having a 3.2-cm diameter with 14,000 Da MW cutoff was soaked in distilled water for 3 h. In a 250-mL glass beaker, about 200 mL of phosphate buffer pH 7.4 containing 2% polysorbate 80 was taken as the release media. The drug and SDs (10 mg) were dispersed in a 5 mL phosphate buffer pH 7.4 in the previously soaked dialysis membrane. The study was conducted on a temperature-controlled magnetic stirrer at 37°C and 60 RPM. At a regular time interval, 2 mL sample was collected and replaced with a fresh medium. These samples were analyzed for concentration using the RP-HPLC method [22].

Ex Vivo Intestinal Permeation/Diffusion Studies

A freshly sacrificed goat ileum was collected from a local slaughterhouse and stored in the Ringer's physiological solution. The ileum was given multiple washings to clean the inner and outer surfaces. Previously dispersed 5 mg drug and 10 mg SDs were taken in goat ileum. The study was conducted in the phosphate buffer of pH 7.4 at 37°C and 60 RPM on a temperature-controlled magnetic stirrer with continuous aeration. At a predetermined time, a 2 mL sample was collected and stored in a refrigerator for further use [22].

Physical Stability Studies

The prepared solid dispersions were stored in a glass desiccator that has $CaCO_3$ crystals to maintain the dry conditions. The desiccator was closed with a lid that contained wax to seal. The desiccator was placed at 25±2°C and 60±5% RH for 60 days, and the samples were collected and analyzed for solubility and drug release [14].

Results and Discussion

MD Simulation Study

The Hildebrand solubility parameter was determined by the MD simulation approach for GLB and selected carriers (Fig. 1). The drug-carrier combination with a higher Hildebrand solubility parameter would give better practical solubility [13]. According to the *in silico* study, GLB-PEG 1500 showed 20.58, whereas GLB-Acconon C-50 showed 16.0 solubility parameter value. Since the GLB-PEG 1500 showed a higher solubility parameter value *in silico* evaluation, the SDs prepared with PEG 1500 would offer better aqueous solubility [4].

Solubility Parameter Approach

The functional group contribution method was used to determine the Hansen solubility parameter for the drug and carriers [5]. The carrier which shows the solubility parameter difference < 7 Mpa1/2 is likely to offer better miscibility [14]. The results for the solubility parameter are given in Table I. According to the Hansen solubility parameter approach, GLB showed 23.46, PEG 1500 showed 47.52, and Acconon C-50 showed 41.23 solubility parameter value in the group contribution method. Therefore, GLB-PEG 1500 SDs may show enhanced solubility than GLB-Acconon C-50 SDs.

Flory-Huggins Interaction Parameters (*x*)

The intimate mixing of drug carrier at higher temperatures leads to the formation of a single phase. This type of physical reaction reduces the melting point of the pure drug, which is known as depression in the melting point. The depression in the melting point can be used to calculate the drug-carrier miscibility [23]. For this, the DSC technique was used. A positive value in x will ultimately lead to amorphous phase separation upon storage [6]. The negative x value indicates the heteronuclear reaction in which the drug and carrier will get adequately mixed. The calculated x value for GLB-PEG 1500 was 0.3861 with R^2 value of 0.93, and x value for GLB-Acconon C-50 was 0.6753 with R^2 value of 0.87. Since the calculated x value for both the carriers with GLB was positive, the chosen carriers would offer limited solubility and may also lead to amorphous separation with GLB in SD formulation.

Gibb's Free Energy Calculation

The *in silico* and Hansen solubility parameters suggested that the GLB would show improved solubility with the selected carriers in SD formulations. In contrast, the Flory-Huggins interaction parameters showed a positive value for both carriers. To understand the miscibility behavior of GLB with PEG 1500 and Acconon C5 0 further, Gibb's free energy was calculated. The different ratios of drug carriers were taken, and the depression in melting point was determined by the DSC technique at the melting temperature of GLB. Gibb's free energy depends on the drug-carrier miscibility (x) and Gibb's free energy gives information about the stability of the

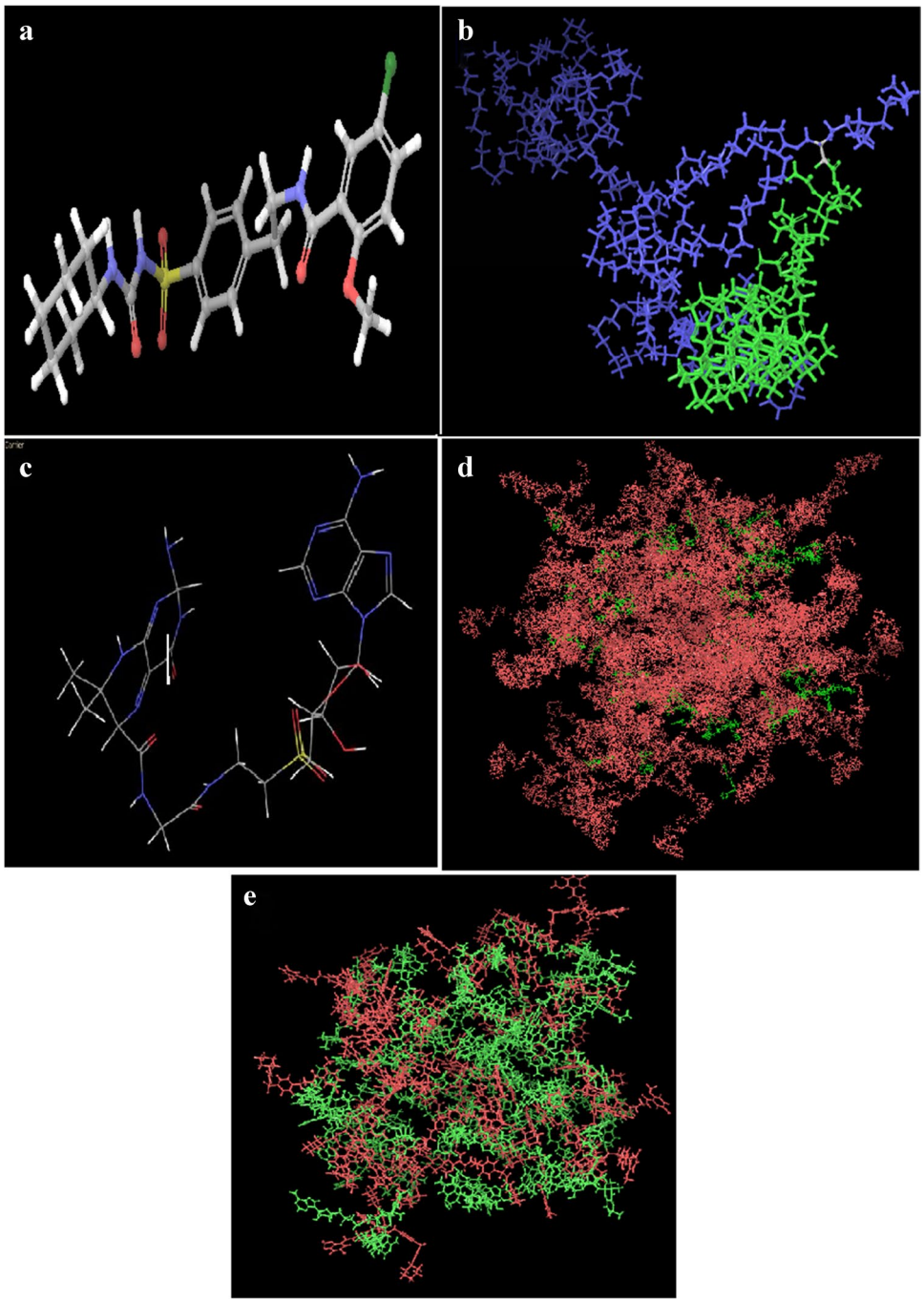

Fig. 1 Computational study 3D structures of various compounds. **a**: GLB; **b**: PEG 1500; **c**: Acconon C-50; **d**: Disorder system GLB-PEG 1500; Disorder system; **e**: Disorder system GLB-Acconon C-50

Table I Hansen Solubility Parameters

Samples	Solubility parameter (δ)
GLB	23.46
PEG 1500	47.52
Acconon C-50	41.23

GLB glibenclamide, *PEG 1500* polyethylene glycol 1500

drug-carrier mix at room temperature [24]. A graph was plotted between drug-carrier weight fraction and ΔG_{mix}(Fig. 2). Since Gibb's free energy depends on the volume fraction, it would suggest an optimum ratio of drug carrier. Beyond the recommended ratio, there might be chances of phase separation or recrystallization upon storage [7]. From the calculated Gibb's free energy data, it was found that there is a negative value for all drug-carrier ratio at the melting point of GLB. Hence, the drug would show miscibility with

selected carriers at particular ratios. One part of GLB can accommodate not more than 4 parts of Acconon C-50 and not more than 2 parts of PEG 1500 without phase separation or recrystallization. After the mentioned value, solid dispersions prepared with GLB-PEG 1500 or GLB-Acconon C-50 would show amorphous phase separation on storage.

Solid-State Characterization

The prepared SDs were analyzed for solid-state characterizations such as DSC, powder X-ray diffraction (PXRD), FTIR, 1H NMR, and microscopic evaluations.

The optical polarized microscopic imaging technique was used to differentiate the crystalline and amorphous compounds. The polarized microscopic image of GLB is given in Fig. 3a, and the images of GLB-PEG 1500 SD, GLB-PEG 1500 ESD, GLB-Acconon C-50 SD, and GLB-Acconon C-50 ESD are shown in Fig. 3b, c, d, and e respectively. Birefringence is an optical property of crystalline materials having a refractive index when the polarized light is passed through them. The crystalline compounds can transmit the polarized light, but the amorphous compounds cannot. Therefore, optical microscopic images give a basic idea of whether the prepared sample is amorphous or crystalline. GLB showed typical birefringence, which confirms that the selected drug is in crystalline form. The birefringence in prepared SDs is reduced, which indicates the crystallinity of GLB is reduced in prepared SDs. This phenomenon is observed more in ESDs. This is because the added effervescent agent might have partially converted the crystalline drug into an amorphous form. The optical polarized microscopic technique is an essential technique to determine the conversion into the amorphous state. To confirm further, PXRD and DSC studies were conducted.

The results of PXRD studies are shown in Fig. 3. A plain X-ray diffractogram of pure GLB revealed that it is crystalline, as indicated by intense peaks (Fig. 3a). The X-ray diffractograms of GLB-PEG 1500 SD, GLB-PEG 1500 ESD, GLB-Acconon C-50 SD, and GLB-Acconon C-50 ESD are shown in Fig. 3b, c, d, and e respectively. The XRD profiles of these SDs indicated the reduction in crystallinity of GLB in their SD and ESD forms. Bragg's peak intensity showed that GLB has not been entirely converted into the amorphous state in the prepared solid dispersions, and SDs showed some portion of crystallinity (Fig. 3). The following formula was used to calculate the extent of conversion to the amorphous state [8].

$$\%Amorphous\ content = \left[1 - \left(\frac{Cumulative\ Bragg's\ intensity\ of\ sample}{Cumulative\ Bragg's\ intensity\ of\ pure\ drug}\right)\right] \times 100$$

From the data collected in PXRD studies, the percentage of amorphous content was higher in ESDs than in SDs, and the results are given in Table II. All ESDs showed improved amorphous content when compared with SDs. The probable reason is the added effervescent agent produces carbonated fizz during the formulation process. The produced fizz promotes the molecular level mixing of dug and carrier. As the molecular level mixing increases, the random distribution of the drug in the polymer matrix will also increase. This ultimately leads to an increase in amorphous nature [10].

To verify these results, the DSC study was conducted (Fig. 4) for GLB, carriers, and SDs [8]. The pure drug showed an endothermic peak at approximately 174°C, indicating its melting point. PEG 1500 recorded a melting point at 60°C, and Acconon C-50 showed a peak at 120°C. The GLB-PEG 1500 SD showed a less intense peak at the melting point of the drug, whereas in the GLB-PEG 1500 ESD, the thermogram was recorded almost as a straight line. A similar kind of pattern was observed in SDs prepared with Acconon C-50. There was an endothermic peak in all SDs at respective carrier melting points. This could be because of improper miscibility of the drug and selected carrier(s) [14]. The positive value in the Flory-Huggins theory and the negative value in Gibb's free energy calculation support the

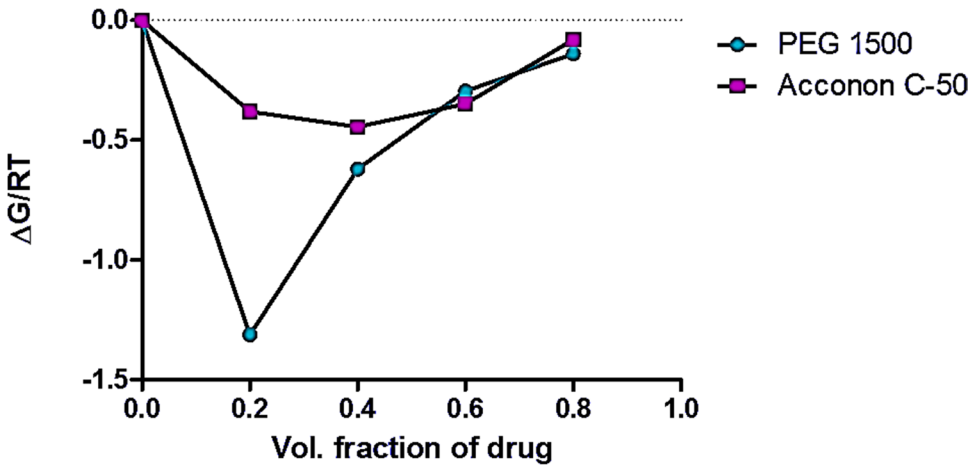

Fig. 2 Gibb's free energy values of GLB carriers

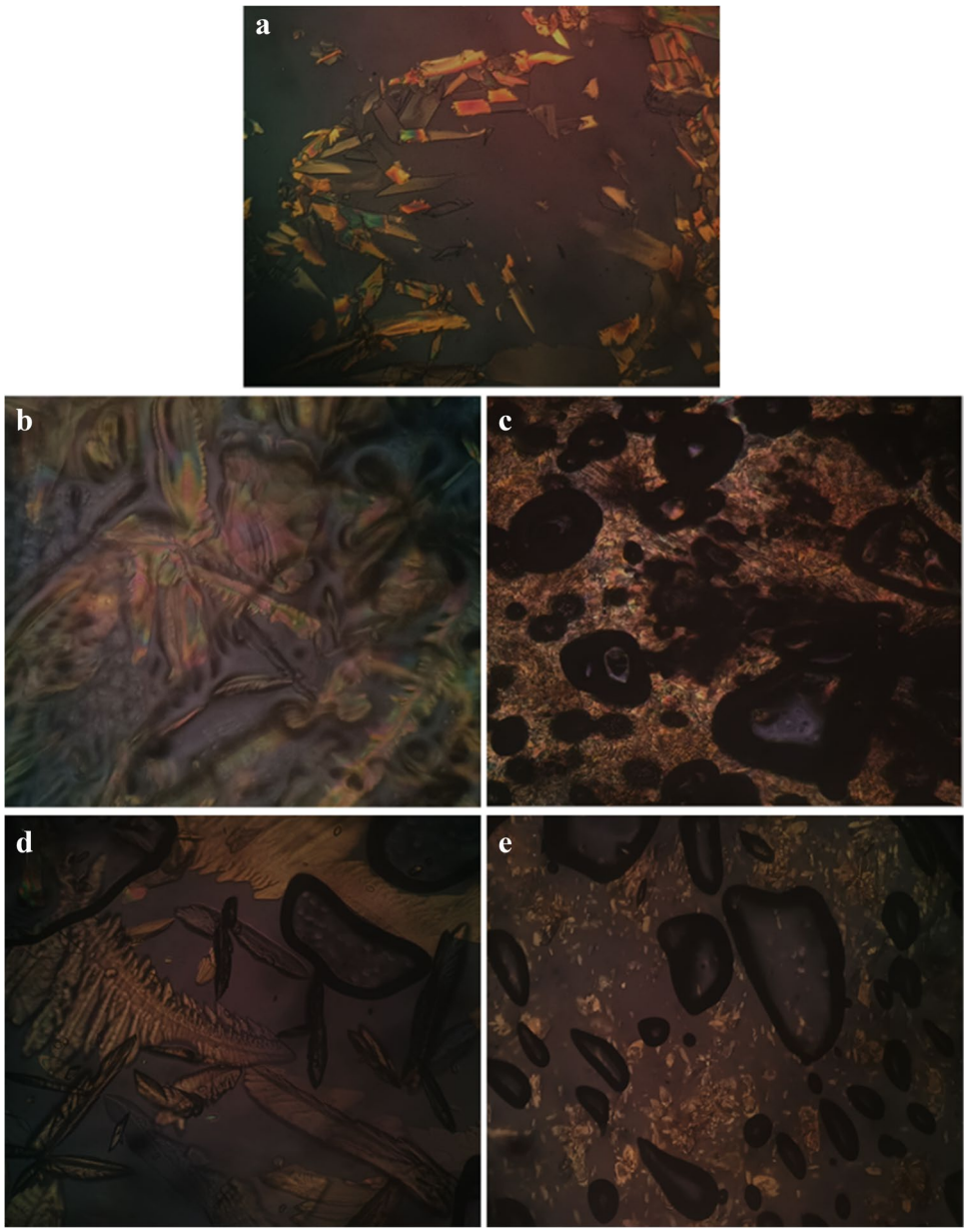

Fig. 3 Polarized microscopic images of SDs and ESDs. **a**. GLB; **b**. GLB-PEG 1500 SD; **c**. GLB-PEG 1500 ESD; **d**. GLB-Acconon C-50 SD; **e**. GLB-Acconon C-50 ESD

improper miscibility of drug and carrier(s) [25]. The Flory-Huggins theory would have shown the negative value if the drug has complete miscibility with the carrier(s). Adding an effervescence agent helped reduce the crystalline nature proved by the PXRD and DSC data.

Table II Percentage Amorphous Content

Solid dispersion	Amorphous content (%)
GLB-PEG 1500 SD	33.93051
GLB-PEG 1500 ESD	52.29887
GLB-Acconon C-50 SD	21.16598
GLB-Acconon C-50 ESD	32.77292

GLB glibenclamide, *PEG 1500* polyethylene glycol 1500, *SD* solid dispersion, *ESD* effervescent solid dispersions

The FTIR spectra were recorded to determine the possible chemical interactions between the drug and the selected carrier(s) (Fig. 5). The FTIR spectrum of physical mixtures of GLB-PEG 1500 and GLB-Acconon C-50 are given in Fig. 5B, C. The peaks in the FTIR spectrum of the pure drug were almost identical to those observed with that of standard [26]. All pure drug functional group peaks are shifted slightly in the drug-carrier physical mix [19]. The benzamide 2° amine has recorded a peak at 3366 cm^{-1} in GLB and GLB-carrier physical mix. The sulphonamide 2° amine recorded a sharp peak at 3314 in pure drug, and it has not moved in the drug-carrier physical mixture. The

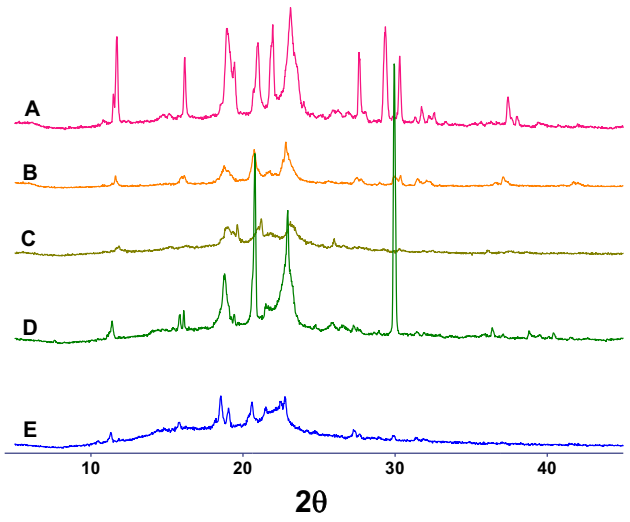

Fig. 4 PXRD patterns of SDs and ESDs. **A** GLB; **B** GLB-PEG 1500 SD; **C** GLB-PEG 1500 ESD; **D** GLB-Acconon C-50 SD; **E** GLB-Acconon C-50 ESD

sulphonyl-carbonyl group recorded a sharp peak at 1713 in the drug and drug-polymer physical mix. The aliphatic –CH in GLB recorded a dual peak at 1310 and 1161, and it remains in the same position in the drug-polymer physical mixture. The –C–Cl showed a peak at 1024 in the drug and drug-carrier physical mixture.

The aryl =CH group recorded a low intense peak at 3317 in pure drug because the aryl=CH group in GLB is surrounded by highly electronegative atoms. In GLB-PEG 1500 physical mix at the same wavenumber, a very low intense peak was recorded. On the other hand, the same functional group has not shown any peak in GLB-Acconon C-50 physical mix due to the strong electronegative environment around the aryl group, making the peak very short. Another reason is that GLB molecules are surrounded by the Acconon C-50 molecules. These reasons make the aryl functional group invisible in GLB-Acconon C-50 physical mixture. This phenomenon is just a physical interaction between drug and carrier.

Moreover, the other functional group peaks neither shifted nor deleted. Hence, there is no chemical incompatibility between the drug and selected carriers. The GLB-PEG 1500 SD, GLB-Acconon C-50 SD, GLB-PEG 1500 ESD, and GLB-Acconon C-50 ESD are given in Fig. 5D, E, F, and G, respectively. The FTIR spectrum in prepared solid dispersions recorded broad peaks with reduced intensity. The probable reason is that the selected carrier's chemical structure and molecular weight are more than the drug's molecular structure. The drug molecules might have been covered by the carrier molecule. The second reason is the drug has functional groups like amide, amine, and sulfonyl, which are strongly involved in the hydrogen bonding with the carriers [27]. The peak broadening was observed more in ESDs than SDs. The added effervescent agent makes the drug more susceptible to hydrogen bonding with the selected carriers. Hence, the ESDs have recorded more broadened peaks than SDs [27].

The results of the FTIR spectra were confirmed by the 1H NMR study. The results of 1H NMR spectroscopic analysis are shown in Fig. 6. In 1H NMR spectroscopy of GLB, the aryl functional group showed 7 protons between 7 and 8 δ values. The methoxy group recorded a singlet peak containing 3 protons at δ value 3. The cyclohexyl and ethylene

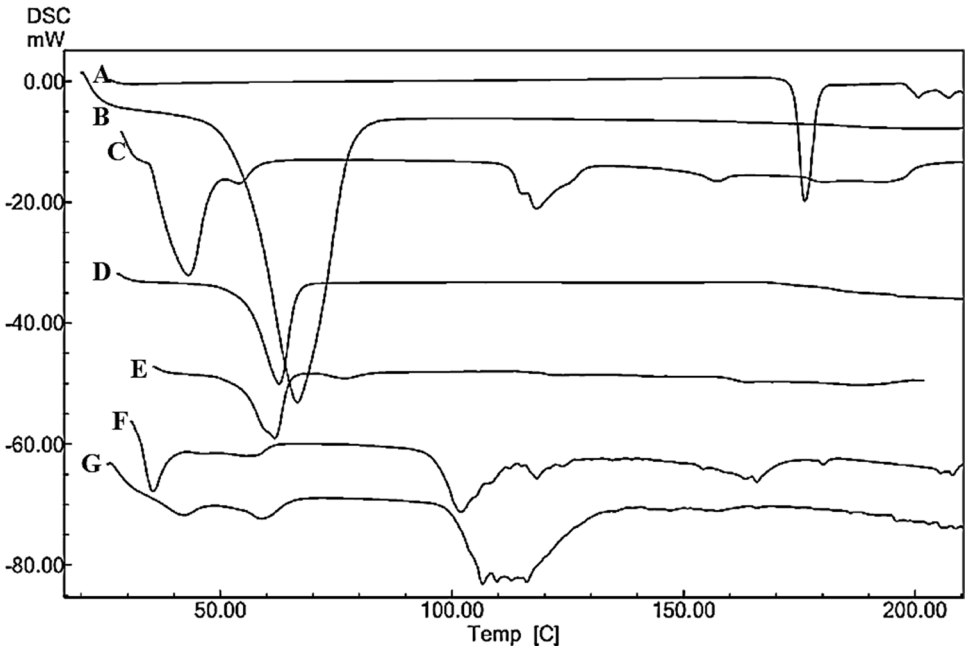

Fig. 5 DSC thermograms of SDs and ESDs. **A** GLB; **B** PEG 1500; **C** Acconon C-50; **D** GLB-PEG 1500 SD; **E** GLB-PEG 1500 ESD; **F** GLB-Acconon C-50 SD; **G** GLB-Acconon C-50 ESD

groups recorded mutilate peaks of 15 protons between 1 and 2 δ value. The amine group recorded two singlet peaks at 6.4 and 6.8 δ value. At the 8.6 δ value, the $–SO_2NH$ recorded a singlet peak [28]. The prepared SDs showed low-intensity peaks with peak broadening. The inter hydrogen bonding between the drug and carrier(s) molecules makes the peak broaden and shifting of peaks to a higher frequency range. This confirms the hydrogen bond formation between the drug and carrier in prepared solid dispersions [28]. The deviation in peak value and peak broadening was more in ESDs than SDs. This is because the added effervescent agent helps in forming hydrogen bonding between the drug and polymer more easily.

The morphology of pure drug and prepared solid dispersions were primarily tested with the motic microscope, and the results are given in Fig. 7. The GLB-PEG 1500 SD and GLB-PEG 1500 ESD motic microscopic images are shown in Fig. 7b, c, respectively. Figure 7d, e shows GLB-Acconon C50 SD and GLB-Acconon C-50 ESD motic microscopic images. From the motic microscopic images, it was found that the pure drug is in crystalline nature (Fig. 7a), and it was observed that the crystalline nature of the pure drug was reduced in the prepared solid dispersions. The conversion into the amorphous form is more in ESDs than SDs. The GLB-Acconon C-50 SD showed more crystalline nature, whereas GLB-PEG 1500 ESDs recorded very low crystallinity

Confirmation of morphology of pure drug and prepared solid dispersions was done using the SEM analysis, and the results are shown in Fig. 8. The SEM data strongly supports the motic microscopic data. Figure 8b shows the morphology of the GLB -PEG 1500 SD. Figure 8c shows the morphology of GLB-PEG 1500 ESD. Morphology of the GLB-Acconon C-50 SD and ESD is given in Fig. 8d, e. From the SEM analysis, it was found that the pure drug is in crystalline form (Fig. 8a).

Further confirmation about the crystallinity of pure drug and prepared SDs was done by the microscopic technique. For this purpose, motic light microscopy and SEM imaging techniques were adopted. Generally, the crystalline materials are in polyhedral shape. The polyhedral shape of the crystalline materials can be viewed under a microscope. From the microscopic data, it was found that the drug is in polyhedral crystalline form. The polyhedral shape crystals were found to be less in prepared SDs. This is because of the partial conversion of the crystalline drug into the amorphous state. The polyhedral shape was found to be less in ESDs than SDs. The probable reason may be added effervescent agent helps in reducing the crystallinity of GLB in ESD formulations. The microscopic images strongly support the XRD and DSC data, which indicated the reduction in crystallinity of the drug in SDs. The crystalline nature was reduced more in ESDs than SDs [29]. The GLB-PEG 1500 ESD showed the lowest crystallinity, whereas the GLB-Acconon C-50 showed the highest crystallinity after the pure GLB [8].

Solubility Studies

Phosphate buffer of pH 6.8 and 7.4 and pH 1.2 acidic buffer were taken as solvents for the solubility study, and the results are given in Fig. 9. GLB showed 0.06 mg/mL in phosphate buffer pH 6.8, 0.08 mg/ mL of solubility in phosphate buffer pH 7.4, and 0.03 mg/mL acidic buffer pH 1.2. The prepared solid dispersions have shown higher solubility in the phosphate buffer pH 7.4 than pH

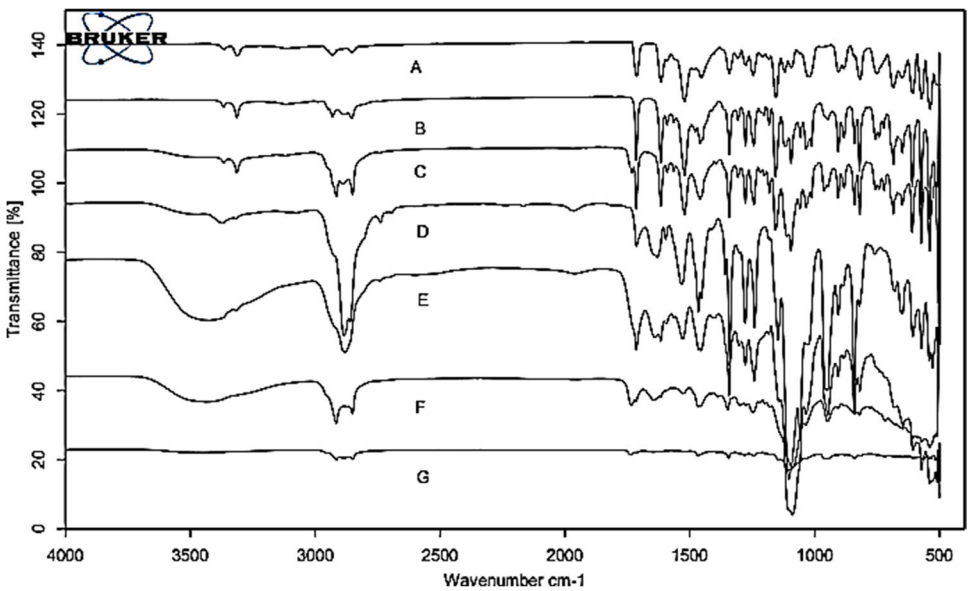

Fig. 6 FTIR spectra of SDs and ESDs. **A** GLB, **B** GLB-PEG 1500 physical mixture, **C** Acconon C-50 physical mixture, **D** GLB-PEG 1500 SD, **E** GLB-Acconon C-50 SD, **F** GLB-PEG 1500 ESD, **G** GLB-Acconon C-50 ESD

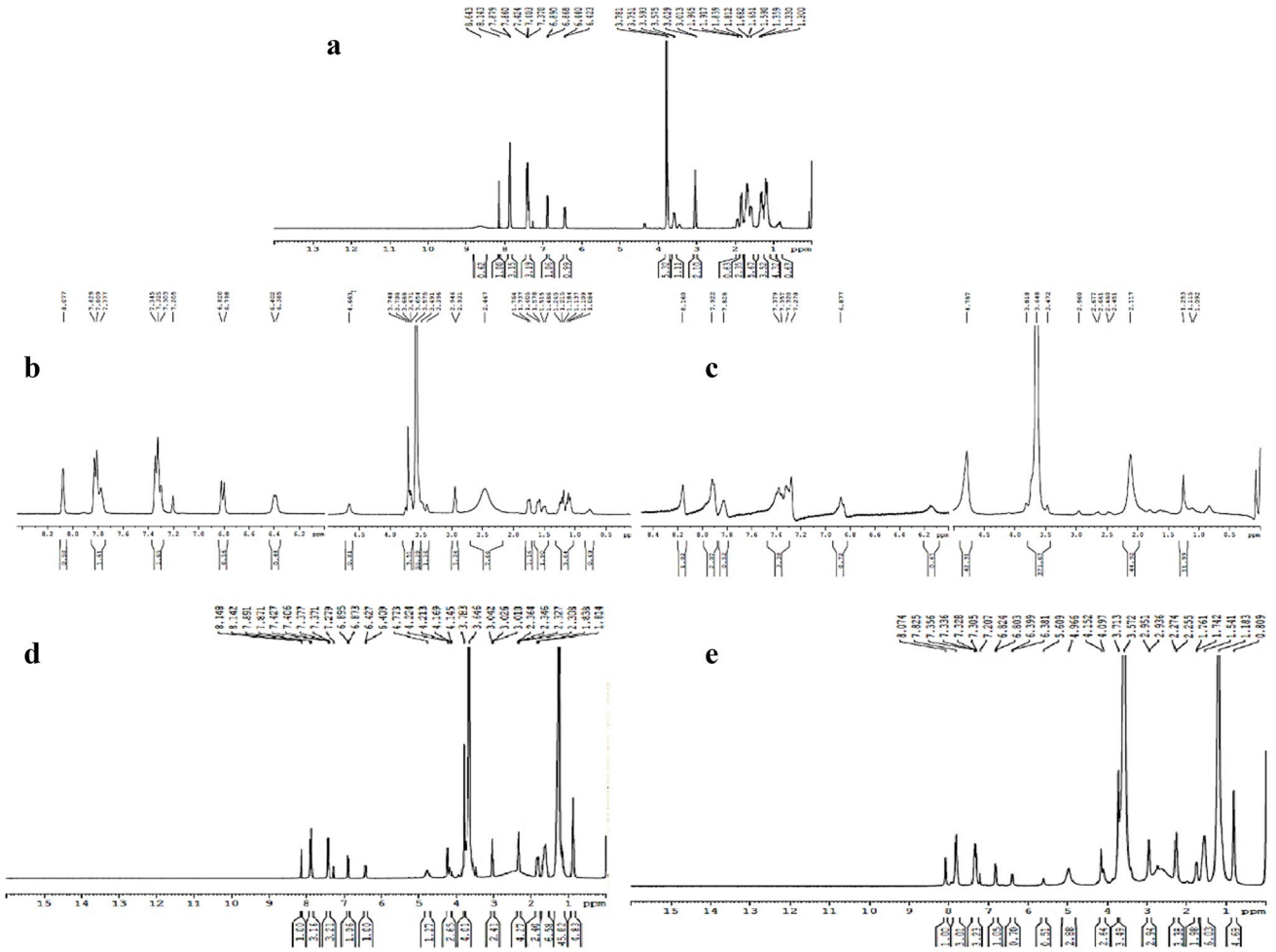

Fig. 7 1H NMR spectra of SDs and ESDs. **a** GLB, **b** GLB-PEG 1500 SD, **c** GLB-PEG 1500 ESD, **d** GLB-Acconon C-50 SD, **e** GLB-Acconon C-50 ESD

6.8 and 1.2 [29]. The probable reason for prepared SDs to show enhanced solubility is improved amorphous nature. Because the amorphous compounds have high free energy, therefore, it is easy for a solvent to convert an amorphous solid to a solution form when compared with a crystalline form. ESDs showed better solubility of the drug than in SDs. The possible reason is sodium citrate molecules in ESDs may change the microenvironmental pH to alkaline since GLB has pH-dependent solubility and absorption [27]. The microwave technique's solid dispersions reported the least solubility, followed by solvent evaporation, lyophilization, and HME [30].

Interestingly, the microwave-assisted GLB-Acconon C-50 ESD recorded the lowest solubility. This is because the effervescence agent has undergone degradation in the presence of microwaves. The HME-assisted GLB-PEG 1500 ESD recorded the maximum solubility, i.e., 3.5 mg/ mL, and microwave-assisted GLB-Acconon C-50 ESD showed 0.34 mg/mL of solubility.

In Vitro Drug Release Studies

The *in vitro* drug release study was performed for GLB, and the prepared solid dispersions in phosphate buffer pH 6.8, 7.4, and acidic buffer pH 1.2, and the results are given in Fig. 10 and Fig. 11. From the dissolution data, it was clearly observed that the drug release was increased with increase in the pH of dissolution media. From the drug release study, it was also found that GLB has shown approximately 16% in pH 7.4, 11.4% in pH 6.8, and 8.4% in pH 1.2 of the drug release at the end of the 90th min. Prepared SDs have also followed the same pattern of drug release. The drug release was enhanced with increase in the pH of the media. The satisfactory release was observed in phosphate buffer pH 7.4. than pH 6.8 and pH 1.2 acidic buffer. Singh *et al*. demonstrated the effect of dissolution media on the dissolution performance of GLB. Authors have proved that the drug release was observed more in phosphate buffer pH 7.4 than in other pH buffers [27]. The solid dispersions prepared using PEG 1500 with all four

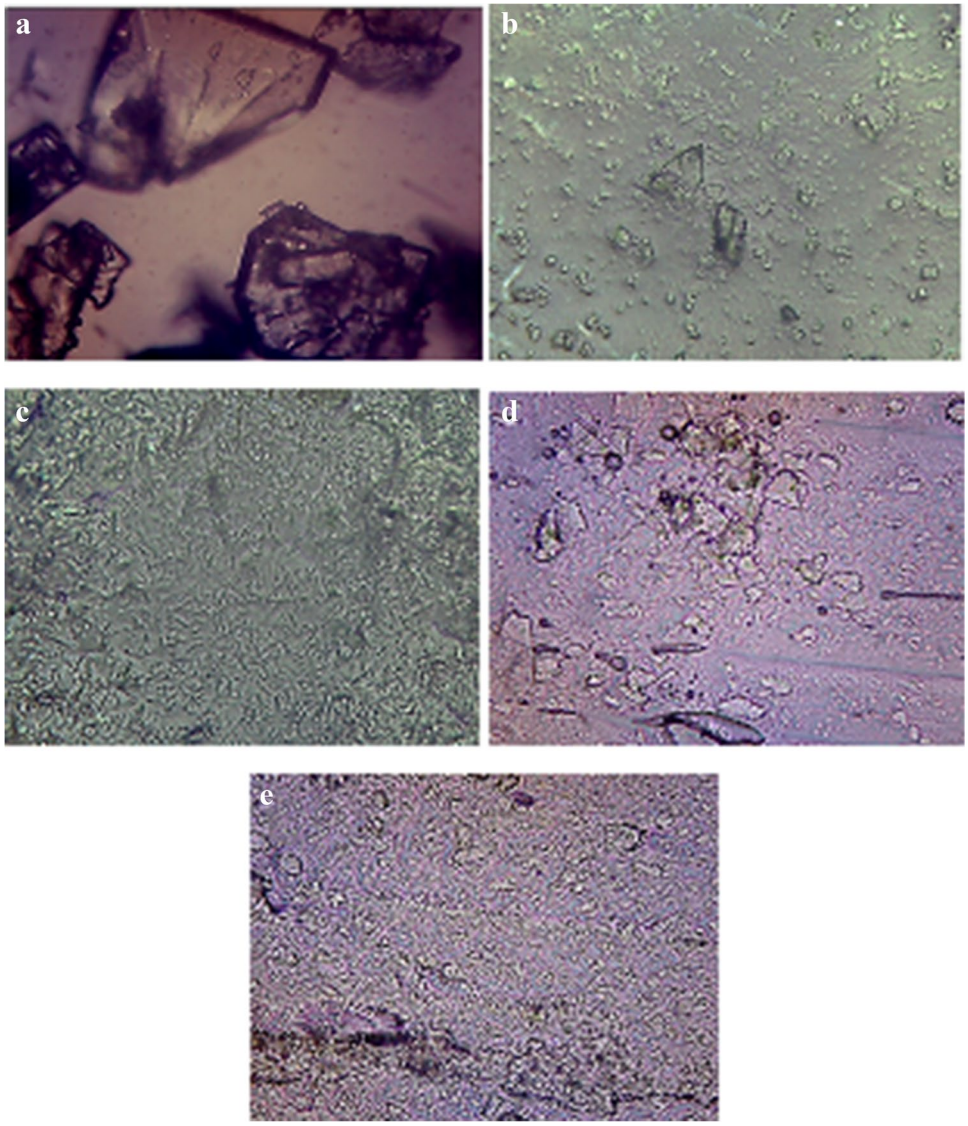

Fig. 8 Microscopic images under motic microscope. **a** GLB, **b** GLB-PEG 1500 SDs, **c** GLB-PEG 1500 ESDs, **d** GLB-Acconon C-50 SDs, **e** GLB-Acconon C-50 SD ESDs

techniques showed an improved dissolution rate compared to solid dispersions prepared with Acconon C-50. GLB-PEG 1500 ESDs prepared using HME recorded the maximum drug release (71%) at the end of the 90th min. Among all SDs, the HME-assisted PEG 1500 SDs showed higher drug release (66%) at the end of the 90 min.

A similar kind of pattern was observed for all ESDs [19]. The ESDs prepared with Acconon C-50 using the microwave technique recorded less solubility (58% at the end of the 90th min). The reason for ESDs showing higher drug release may be due to the presence of a higher proportion of the drug in the amorphous form in ESDs than in SDs. The atoms in the amorphous form are arranged irregularly in 3D space, due to which the dissolution media can quickly enter into the amorphous solids and convert them into solution. The second reason could be that GLB has pH-dependent solubility. The added effervescent agent can change the microenvironmental pH to alkaline, which enhances the solubility of GLB in ESDs. However, with respect to the SDs produced by the microwave irradiation method, the solubility and dissolution rate were not much appreciated compared to the SDs prepared by other methods in this study. The reason for this is that the use of microwave radiation might have degraded the effervescent salt partially, due to which its solubility got affected, which led to a reduction in the dissolution rate [30].

In Vitro Diffusion and *Ex Vivo* Intestinal Permeation Studies

GLB is a BSC-II drug and has none of the permeability issues. But, the solid dispersions come under the colloidal systems whose particle size is not similar, which will affect the dissolution and permeability. So, measuring permeability across the membrane is equally important [14]. The

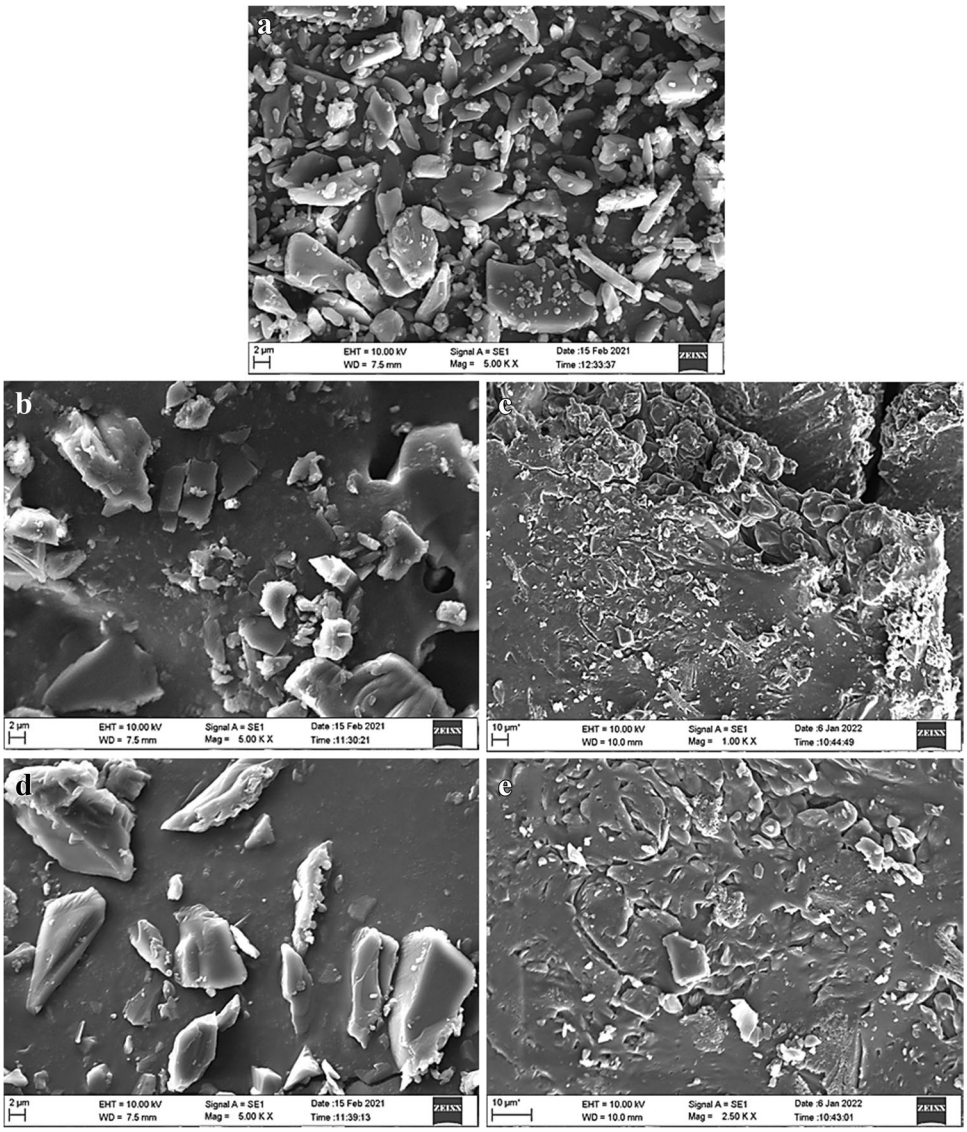

Fig. 9 Scanning electron microscopic images of SDs and ESDs. **a** GLB, **b** GLB -PEG 1500 SDs, **c** GLB-PEG 1500 ESDs, **d** GLB-Acconon C-50 SDs, **e** GLB-Acconon C-50 SD ESDs

in vitro flux was determined using the dialysis membrane method. To mimic the biological conditions, intestinal tissue was used in a separate study. Since SDs prepared by HME recorded the maximum solubility and dissolution rate, an *in vitro* diffusion and e*x vivo* permeation study were performed [21]. Table III shows the *in vitro* diffusion and e*x vivo* permeation study results of plain GLB and the prepared SDs. The plain GLB recorded 0.15 µg/cm^2/min. The GLB-PEG 1500 SD showed 0.54, and GLB-PEG 1500 ESD showed 1.31 µg/cm^2/min. The GLB-Acconon C SDs recorded 0.67 µg/cm^2/min, whereas the GLB-Acconon C ESDs recorded 1.65µg/cm^2/min.

Taylor *et al*. [31] demonstrated that the flux depends on the drug dissolved in the release media. The drug should have an optimum hydrophilic and lipophilic balance to cross the biological membrane. Though the SDs prepared by PEG 1500 showed higher solubility and drug release, the SDs prepared by GLB-Acconon C-50 SDs showed better flux *in vitro* and *ex vivo* permeation studies. The possible reason is that the PEG 1500 has higher surfactant property than Acconon C-50. Hence, it can form micelles and enhance the permeability across the membrane [10, 32]. From the flux calculations, it was also found that the ESDs have shown better flux than SDs. This is because sodium citrate has the property of enhancing permeability across the biological membrane. Hence, the ESDs recorded higher flux than SDs [11].

The *in vitro* and *in vivo* correlation (IVIVC) is an essential step in deciding the bioavailability of the drugs. The novel formulations that improved solubility and dissolution rate failed to enhance the bioavailability because of improper IVIVC. To mimic IVIVC, Bao *et al*. [28] demonstrated the *in vitro-ex vivo* correlation (IVEVC) method. According to Blakney *et al*., there are several methods to determine the

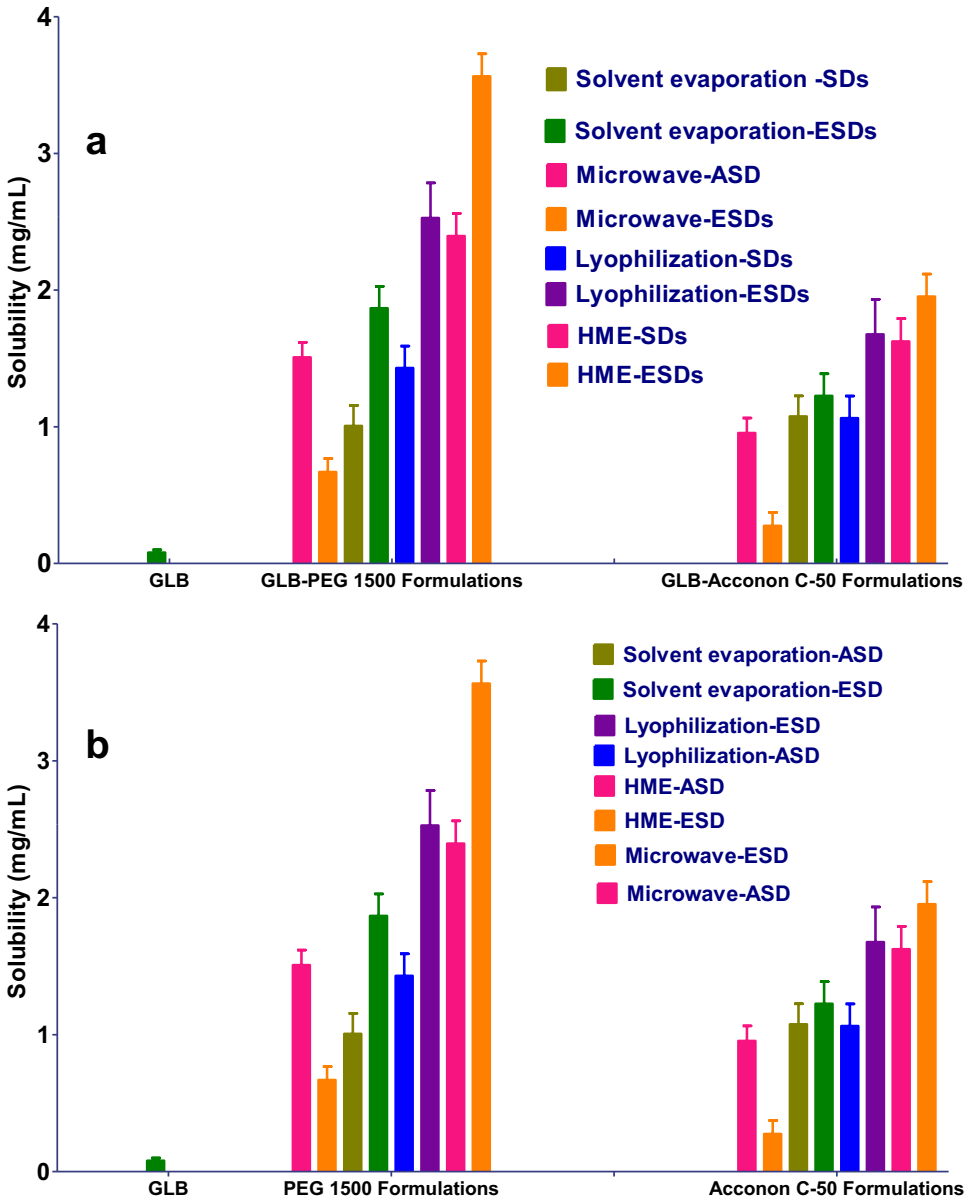

Fig. 10 Solubility study of drug and SDs, ESDs in different buffers. **a** Phosphate buffer pH 7.4, **b** Phosphate buffer pH 6.8. The results are presented as mean±SD, *n*=3

IVEVC. The regression coefficient method is easier and less time-consuming. For this purpose, a graph plotted between the *in vitro* and *ex vivo* flux and its R^2 was measured. The formulation whose R^2 is close to 1 can be considered to have a good IVEVC [33]. IVEVC was measured for GLB and SDs prepared by HME, and the results are given in Table IV. The R^2 for GLB was 0.69, and GLB-Acconon C-50 ESD prepared by HME showed an R^2 of 0.96. This is because the surfactant nature of the Acconon C-50 and added effervescent salts helped increase cell permeability [10].

Table III The Flux Values Obtained from *In Vitro* Diffusion Studies and *Ex Vivo* Intestinal Permeation Studies

GLB carrier	Flux (μg/cm^2/min)			
	In vitro		*Ex vivo*	
	SD	ESD	SD	ESD
GLB	0.1513		0.2566	
GLB-PEG 1500	0.54	1.31	0.43	0.92
GLB-Acconon C	0.67	1.65	0.75	1.84

GLB glibenclamide, *PEG 1500* polyethylene glycol 1500, *SD* solid dispersion, *ESD* effervescent solid dispersions

Physical Stability

The solid dispersions prepared by HME were exposed to 25±2°C and 60±5% RH for 60 days. The samples were collected and analyzed for solubility and dissolution rate, and the results are shown in Figs. 12 and 13 [21]. The GLB-PEG 1500 ESD showed 3.5 and 3.14 mg/mL solubility before the stability

Table IV *In Vitro-Ex Vivo* Correlation of GLB and SDs by Regression Coefficient Value

GLB carrier	Regression coefficient	
	SD	ESD
GLB	0.6529	
GLB-PEG 1500	0.90	0.93
GLB-Acconon C-50	0.8948	0.96

GLB glibenclamide, *PEG 1500* polyethylene glycol 1500, *SD* solid dispersion, *ESD* effervescent solid dispersions

study. The same formulation showed 3.1 mg/mL solubility in phosphate buffer pH 7.4 after the stability studies. The GLB-PEG 1500 ESD recorded 65% and 58% before and after stability studies. From the stability data, it was found that there is no much deviation in the solubility and dissolution rate observed from the results after the physical stability. This could be because of three reasons. The first reason is that the melting value for the prepared solid dispersions is more than the storage temperature (25°C). Sailaja *et al*. [34] explained that the chances of phase separation or recrystallization are significantly

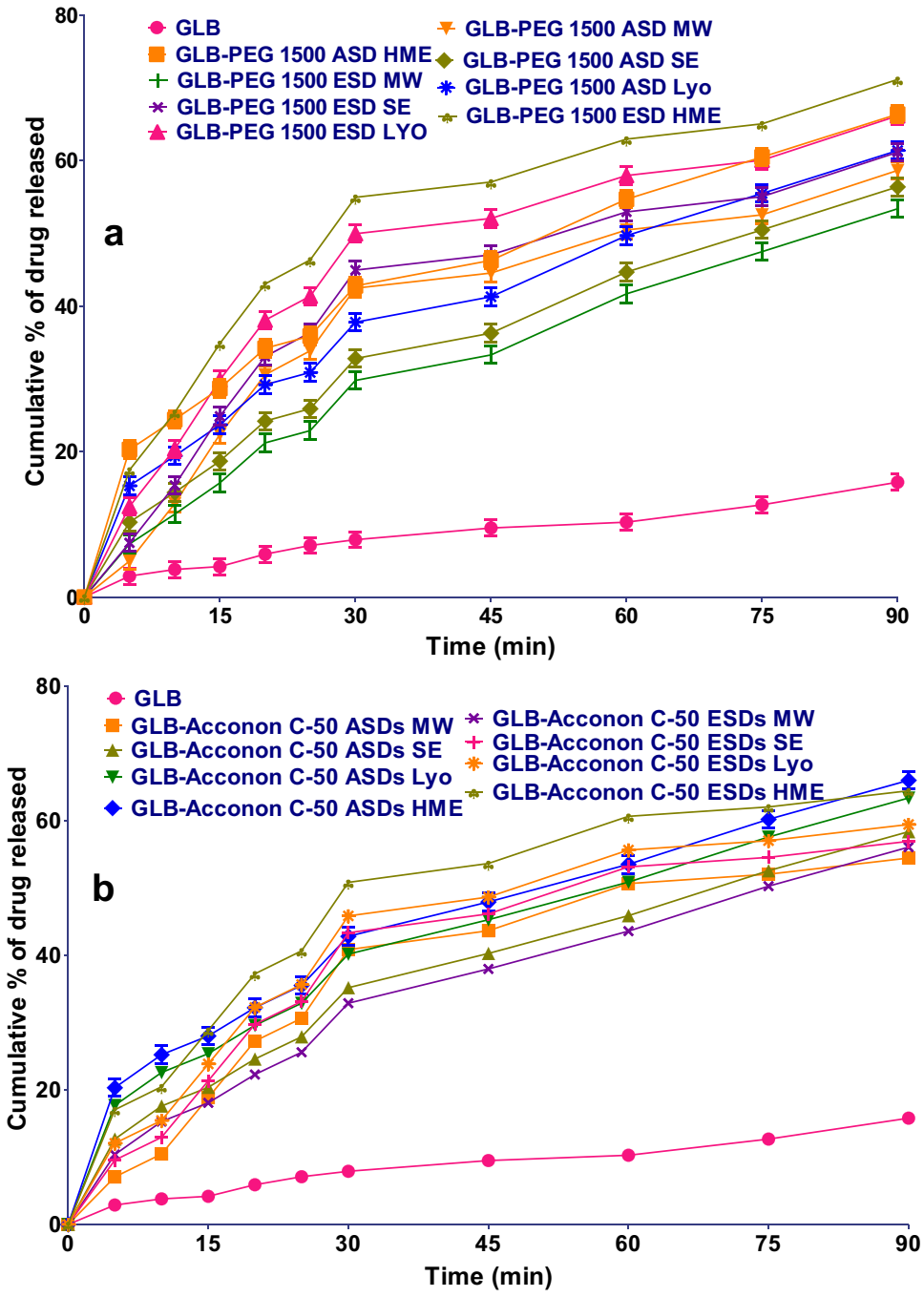

Fig. 11 Cumulative drug release of GLB, SDs and ESDs. **a**: GLB-PEG 1500 solid dispersions; **b**: GLB-Acconon C-50 solid dispersion. The results are presented as mean±SD, n=3. MW microwave, SE solvent evaporation, Lyo lyophilization, HME hot melt extrusion

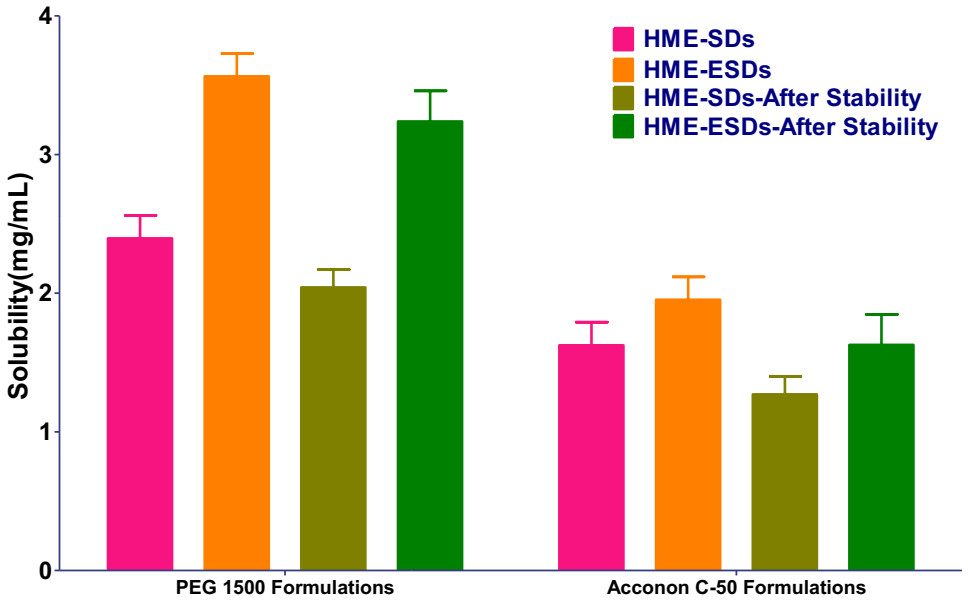

Fig. 12 Solubility profiles of GLB, SDs, and ESDs after stability study. The results are presented as mean±SD, n=3

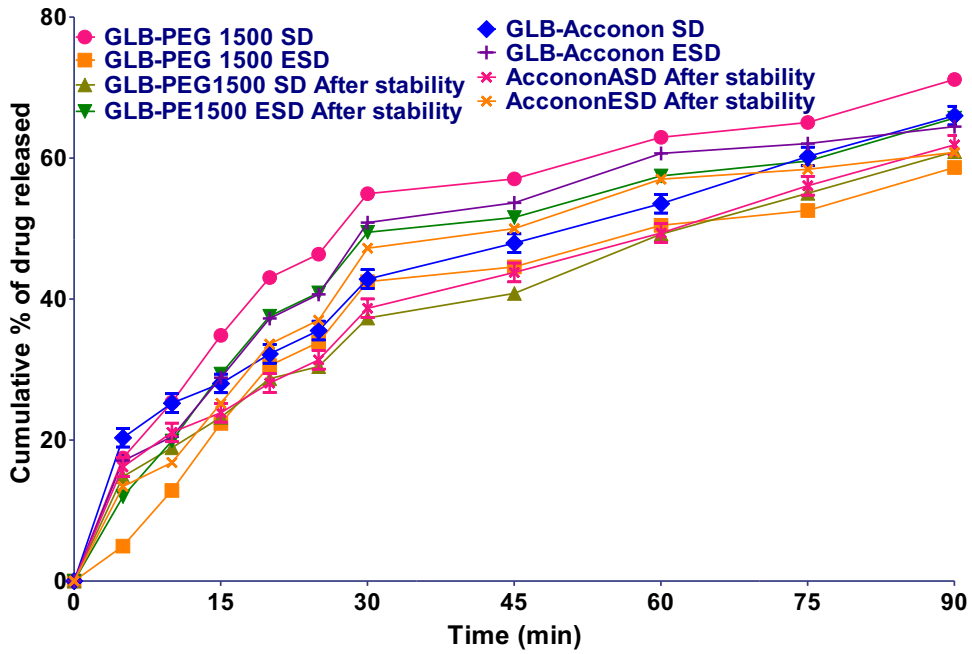

Fig. 13 *In vitro* drug release profiles of GLB from different samples after stability study. The results are presented as mean±SD, n=3

less for the materials with a higher melting point and T_g than the storage conditions. The prepared solid dispersions have not been affected much by the storage conditions since these have a higher melting point than the storage temperature. The second reason is that the drug and carrier might have mixed at the molecular level, due to which the drug might have frozen into the carrier. Therefore, there will not be any thermodynamic push to initiate the crystal growth [21, 35]. The third reason is that GLB might be converted into polymorphic forms upon exposure to temperature and humidity. The polymorphic form of GLB has proved to have improved solubility than the pure GLB [36]. These are the probable reasons for the unusual results after the stability experiment, which might require a detailed study to confirm further.

Conclusion

The current study aimed to investigate the miscibility of GLB with PEG 1500 and Acconon C-50 in pharmaceutical solid dispersions. The drug-carrier(s) miscibility was investigated primarily using the *in silico* molecular dynamic

simulation approach and then by Hansen solubility. To know the further miscibility of the drug with the selected carrier(s), Flory-Huggins miscibility parameters were calculated. The results of *in silico* molecular dynamic simulation, Hansen solubility, suggested that the drug would show good solubility in SDs. To improve the amorphous nature, solubility, and drug release further, the effervescent technique was introduced. The solid dispersions were prepared by microwave, solvent evaporation, lyophilization, and hot-melt extrusion techniques. The amorphous nature was induced successfully by these methods. Among all the methods, microwave technology was less effective. The hydrogen bonding between the drug and carriers was confirmed by FTIR and 1H NMR. The DSC, PXRD, and microscopic imaging techniques proved the conversion of GLB into the partial amorphous form. The transformation to the amorphous form was comparatively higher in ESDs. This improvement in the amorphous nature directly affected the solubility, drug release, and the *in vitro* and *ex vivo* flux values. Therefore, introducing an effervescent agent would help to improve the amorphous nature, solubility, drug release, and stability of conventional solid dispersions.

Acknowledgements The authors are thankful to Sun Pharmaceutical Industries Ltd (Ahmedabad, India) for providing glibenclamide, Unitop Chemicals Private Limited (Thane, India) for providing polyethylene glycol (PEG) 1500, and ABITEC Corporation (Mumbai, India) for providing Acconon C-50 as gift samples. The authors also thank Steer Life Private Limited (Bangalore), Manipal College of Pharmaceutical Sciences and Manipal Academy of Higher Education, Manipal for providing the facilities.

Author Contribution MP: methodology, writing the original draft. VBK: analysis and interpretation FTIR and 1H NMR data. CHM: analysis of *in silico* molecular dynamics simulation study. UYN: interpretation of *in silico* molecular dynamics simulation. KBK: ideology and supervision. SM: ideology, methodology, supervision, original draft editing.

Funding Open access funding provided by Manipal Academy of Higher Education, Manipal

Declarations

Conflict of Interest The authors declare no competing interests.

References

1. Gurunath S, Pradeep Kumar S, Basavaraj NK, Patil PA. Amorphous solid dispersion method for improving oral bioavailability of poorly water-soluble drugs. J Pharm Res [Internet]. Elsevier Ltd; 2013;6:476–80. Available from: https://doi.org/10.1016/j.jopr.2013.04.008.
2. Tran P, Pyo YC, Kim DH, Lee SE, Kim JK, Park JS. Overview of the manufacturing methods of solid dispersion technology for improving the solubility of poorly water-soluble drugs and application to anticancer drugs. Pharmaceutics. 2019;11:1–26.
3. Gao P, Shi Y. Characterization of supersaturatable formulations for improved absorption of poorly soluble Drugs. AAPS J. 2012;14:703–13.
4. Mehta CH, Narayan R, Aithal G, Pandiyan S, Bhat P, Dengale S, *et al*. Molecular simulation driven experiment for formulation of fixed dose combination of Darunavir and Ritonavir as anti-HIV nanosuspension. J Mol Liq [Internet]. Elsevier B.V.; 2019;293:111469. Available from: https://doi.org/10.1016/j.molliq.2019.111469.
5. Yani Y, Kanaujia P, Chow PS, Tan RBH. Effect of API-polymer miscibility and interaction on the stabilization of amorphous solid dispersion: a molecular simulation study. Ind Eng Chem Res. 2017;56:12698–707.
6. Li S, Tian Y, Jones DS, Andrews GP. Optimising drug solubilisation in amorphous polymer dispersions: rational selection of hot-melt extrusion processing parameters. AAPS PharmSciTech. 2016;17:200–13.
7. Jaafar MA, Rousse DR, Gibout S, Bédécarrats JP. A review of dendritic growth during solidification: mathematical modeling and numerical simulations. Renew Sustain Energy Rev [Internet]. Elsevier Ltd; 2017;74:1064–79. Available from: https://doi.org/10.1016/j.rser.2017.02.050.
8. Raghavendra HL, Kumar GP. Development and evaluation of polymer-bound glibenclamide oral thin film. J Bioequiv Availab. 2016;09:324–30.
9. Heo MY, Piao ZZ, Kim TW, Cao QR, Kim A, Lee BJ. Effect of solubilizing and microemulsifying excipients in polyethylene glycol 6000 solid dispersion on enhanced dissolution and bioavailability of ketoconazole. Arch Pharm Res. 2005;28:604–11.
10. Patel N, Dalrymple DM, Serajuddin ATM. Development of solid SEDDS, III: application of Acconon® C-50 and Gelucire® 50/13 as both solidifying and emulsifying agents for medium chain triglycerides. J Excipients Food Chem. 2012;3:83–92.
11. Alam MA, Al-Jenoobi FI, Al-Mohizea AM, Ali R. Effervescence assisted fusion technique to enhance the solubility of drugs. AAPS PharmSciTech. 2015;16:1487–94.
12. Han X, Wang M, Ma Z, Xue P, Wang Y. A new approach to produce drug nanosuspensions CO2-assisted effervescence to produce drug nanosuspensions. Colloids Surfaces B Biointerfaces [Internet]. Elsevier B.V.; 2016;143:107–10. Available from: https://doi.org/10.1016/j.colsurfb.2016.03.017.
13. Chan TI, Ouyang D. Investigating the molecular dissolution process of binary solid dispersions by molecular dynamics simulations. Asian J Pharm Sci [Internet]. Elsevier B.V.; 2018;13:248–54. Available from: https://doi.org/10.1016/j.ajps.2017.07.011.
14. Lakshman D, Chegireddy M, Hanegave GK, Sree KN, Kumar N, Lewis SA, *et al*. Investigation of drug-polymer miscibility, biorelevant dissolution, and bioavailability improvement of Dolutegravir-polyvinyl caprolactam-polyvinyl acetate-polyethylene glycol graft copolymer solid dispersions. Eur J Pharm Sci [Internet]. Elsevier B.V.; 2020;142:105137. Available from: https://doi.org/10.1016/j.ejps.2019.105137.
15. Moneghini M, De Zordi N, Solinas D, MacChiavelli S, Principalle F. Characterization of solid dispersions of itraconazole

and vitamin e TPGS prepared by microwave technology. Future Med Chem. 2010;2:237–46.
16. Meng F, Trivino A, Prasad D, Chauhan H. Investigation and correlation of drug polymer miscibility and molecular interactions by various approaches for the preparation of amorphous solid dispersions. Eur J Pharm Sci [Internet]. Elsevier B.V.; 2015;71:12–24. Available from: https://doi.org/10.1016/j.ejps.2015.02.003.
17. Betageri GV, Makarla KR. Enhancement of dissolution of glyburide by solid dispersion and lyophilization techniques. Int J Pharm. 1995;126:155–60.
18. Frank KJ, Rosenblatt KM, Westedt U, Hölig P, Rosenberg J, Mägerlein M, *et al*. Amorphous solid dispersion enhances permeation of poorly soluble ABT-102: true supersaturation vs. apparent solubility enhancement. Int J Pharm [Internet]. Elsevier B.V.; 2012;437:288–93. Available from: https://doi.org/10.1016/j.ijpharm.2012.08.014.
19. Chen XQ, Ziemba T, Huang C, Chang M, Xu C, Qiao JX, *et al*. Oral delivery of highly lipophilic, poorly water-soluble drugs: self-emulsifying drug delivery systems to improve oral absorption and enable high-dose toxicology studies of a cholesteryl ester transfer protein inhibitor in preclinical species. J Pharm Sci [Internet]. American Pharmacists Association; 2018;107:1352–60. Available from: https://doi.org/10.1016/j.xphs.2018.01.003.
20. Blaabjerg LI, Bulduk B, Lindenberg E, Löbmann K, Rades T, Grohganz H. Influence of glass forming ability on the physical stability of supersaturated amorphous solid dispersions. J Pharm Sci. 2019;108:2561–9.
21. Sai Krishna Anand V, Sakhare SD, Navya Sree KS, Nair AR, Raghava Varma K, Gourishetti K, *et al*. The relevance of co-amorphous formulations to develop supersaturated dosage forms: in-vitro, and ex-vivo investigation of Ritonavir-Lopinavir co-amorphous materials. Eur J Pharm Sci. 2018;123:124–34.
22. Bhargav E, Chaithanya Barghav G, Padmanabha Reddy Y, Pavan kumar C, Ramalingam P, Haranath C. A Design of Experiment (DoE) based approach for development and optimization of nano-suspensions of telmisartan, a BCS class II antihypertensive drug. Futur J Pharm Sci. 2020;6.
23. Moseson DE, Taylor LS. The application of temperature-composition phase diagrams for hot melt extrusion processing of amorphous solid dispersions to prevent residual crystallinity. Int J Pharm [Internet]. Elsevier B.V.; 2018;553:454–66. Available from: https://doi.org/10.1016/j.ijpharm.2018.10.055.
24. Mamidi HK, Rohera BD. Application of thermodynamic phase diagrams and Gibbs free energy of mixing for screening of polymers for their use in amorphous solid dispersion formulation of a non-glass-forming drug. J Pharm Sci [Internet]. Elsevier Inc.; 2021;110:2703–17. Available from: https://doi.org/10.1016/j.xphs.2021.01.036.
25. Mamidi HK, Rohera BD. Material-sparing approach using differential scanning calorimeter and response surface methodology for process optimization of hot-melt extrusion. J Pharm Sci [Internet]. Elsevier Inc.; 2021;110:3838–50. Available from: https://doi.org/10.1016/j.xphs.2021.08.031.
26. Silva Filho SF, Pereira AC, Sarraguça JMG, Sarraguça MC, Lopes J, Façanha Filho P de F, *et al*. Synthesis of a glibenclamide cocrystal: full spectroscopic and thermal characterization. J Pharm Sci [Internet]. American Pharmacists Association; 2018;107:1597–604. Available from: https://doi.org/10.1016/j.xphs.2018.01.029.
27. Kapourani A, Valkanioti V, Kontogiannopoulos KN, Barmpalexis P. Determination of the physical state of a drug in amorphous solid dispersions using artificial neural networks and ATR-FTIR spectroscopy. Int J Pharm X [Internet]. Elsevier B.V.; 2020;2:100064. Available from: https://doi.org/10.1016/j.ijpx.2020.100064.
28. Baghel S, Cathcart H, O'Reilly NJ. Understanding the generation and maintenance of supersaturation during the dissolution of amorphous solid dispersions using modulated DSC and 1H NMR. Int J Pharm [Internet]. Elsevier B.V.; 2018;536:414–25. Available from: https://doi.org/10.1016/j.ijpharm.2017.11.056.
29. Singh S, Srinivasan K, Gowthamarajan K, Narayan G. Development and validation of discriminatory dissolution procedure for poorly soluble glyburide. Asian J Pharm. 2010;4:205–12.
30. Zia J, Riyazuddin M, Aazam ES, Riaz U. Rapid catalytic degradation of amoxicillin drug using ZnFe2O4/PCz nanohybrids under microwave irradiation. Mater Sci Eng B Solid-State Mater Adv Technol [Internet]. Elsevier; 2020;261:114713. Available from: https://doi.org/10.1016/j.mseb.2020.114713.
31. Raina SA, Zhang GGZ, Alonzo DE, Wu J, Zhu D, Catron ND, *et al*. Enhancements and limits in drug membrane transport using supersaturated solutions of poorly water soluble drugs. J Pharm Sci [Internet]. Elsevier Masson SAS; 2014;103:2736–48. Available from: https://doi.org/10.1002/jps.23826.
32. Panigrahi KC, Patra CN, Jena GK, Ghose D, Jena J, Panda SK, *et al*. Gelucire: a versatile polymer for modified release drug delivery system. Futur J Pharm Sci [Internet]. Elsevier Ltd; 2018;4:102–8. Available from: https://doi.org/10.1016/j.fjps.2017.11.001.
33. Blakney AK, Little AB, Jiang Y, Woodrow KA. In vitro-ex vivo correlations between a cell-laden hydrogel and mucosal tissue for screening composite delivery systems. Drug Deliv. 2017;24:582–90.
34. Sailaja U, Thayyil MS, Kumar NSK, Govindaraj G. Molecular dynamics of amorphous pharmaceutical fenofibrate studied by broadband dielectric spectroscopy. J Pharm Anal [Internet]. Elsevier; 2016;6:165–70. Available from: https://doi.org/10.1016/j.jpha.2014.09.003.
35. Papadimitriou SA, Barmpalexis P, Karavas E, Bikiaris DN. Optimizing the ability of PVP/PEG mixtures to be used as appropriate carriers for the preparation of drug solid dispersions by melt mixing technique using artificial neural networks: I. Eur J Pharm Biopharm [Internet]. Elsevier B.V.; 2012;82:175–86. Available from: https://doi.org/10.1016/j.ejpb.2012.06.003.
36. Thongnopkoon T, Puttipipatkhachorn S. New metastable form of glibenclamide prepared by redispersion from ternary solid dispersions containing polyvinylpyrrolidone-K30 and sodium lauryl sulfate. Drug Dev Ind Pharm. 2016;42:70–9.